

*Supplemental Information*

**Biochar colloids act as both transporters of organic pollutants and stimulants of respiratory chain electron efflux: a new understanding of microbial degradation of adsorbed pollutants**

Zhongmiao Wang,<sup>a</sup> Jie Hou,<sup>a</sup> Jiang Xu,<sup>a</sup> Kun Yang,<sup>a</sup> and Daohui Lin<sup>a,b,\*</sup>

<sup>a</sup> Zhejiang Provincial Key Laboratory of Organic Pollution Process and Control, Department of Environmental Science, Zhejiang University, Hangzhou 310058, China

<sup>b</sup> Zhejiang Ecological Civilization Academy, Anji 313300, China

\*Corresponding author: [lindaohui@zju.edu.cn](mailto:lindaohui@zju.edu.cn) (D. Lin)

Number of pages: 14

Number of texts: 6

Number of tables: 2

Number of figures:10

### **Text S1. Resuscitation and culture of bacteria**

The methodology involved isolation of single colonies of TG9 from agar plates followed by incubation in LB liquid medium at 30°C and 180 rpm for 1.5 days. Subsequently, 0.5 mL of the bacterial culture was transferred to fresh LB medium and incubated under identical conditions for 24 h. Upon reaching turbidity (OD<sub>600</sub>=0.7-1.0), 0.5 mL of the culture was transferred to fresh LB medium supplemented with 20 mg/L biphenyl, and further incubated under the same conditions to induce the bacterium's ability to degrade PCBs.<sup>1, 2</sup> Upon reaching the logarithmic growth phase (approximately 24 h of incubation), bacterial cells were harvested by centrifugation at 4000 rpm for 10 minutes. The pellet was then washed three times with saline to remove residual LB medium, and the cells were resuspended in inorganic salt medium for subsequent experiments. TG9 cultures were maintained on LB agar plates and subcultured every two weeks to sustain bacterial viability. All media used in this study were autoclaved at 120°C for 20 minutes, and the compositions of the inorganic salt media are detailed in **Table S1**.

### **Text S2. Determination of supernatant PCB28 and biomass for kinetic experiments.**

After the incubation, the supernatant was centrifuged at 4000 rpm for 45 min, the same volume of n-hexane was added to the supernatant, and the PCB28 was extracted by vortexing the supernatant at 2500 rpm for 2 min.<sup>3</sup> The desorption of the adsorbed PCB28 was evaluated after measuring the concentration of PCB28 in the supernatant.

The bacteria were gradually diluted to 10<sup>7</sup>-10<sup>8</sup> CFU with saline, and the diluted bacterial solution was evenly dispersed on the surface of LB solid medium using the glass bead spreading method, and the change value of biomass was calculated after the single colony had grown. The change in biomass is calculated using the following equation.

$$\text{Variation in total colony count} = \frac{CFU_t}{CFU_{initial}}$$

where  $CFU_{initial}$  represents the biomass of bacteria in the system at 0 day, and  $CFU_t$  denotes the biomass of bacteria in the system after  $t$  days. In this experiment, each group consists of four replicates, with three plates per replicate.

### **Text S3. Instrumental determination parameters of PCBs and degradation products**

The concentration of PCB28 was determined using the following GC-ECD procedure.<sup>4</sup> Initially, the column oven temperature was set to 120°C and maintained for 1 min; subsequently, the temperature was ramped up to 200°C at a rate of 35°C per min; then, it was further increased to 204°C at a rate of 2°C per min; at the final stage, the temperature was raised to 295°C at a rate of 10°C per min and held for 2 min. The inlet temperature was set at 250°C, while the detector temperature was set at 300°C. A volume of 4.0 µL was injected, and the detection limit was determined to be 10 ng/L.

In the GC-MS analysis, a Shimadzu capillary column (SH-Rxi-5Sil MS, 30.0 m×0.25 mm×0.25 µm) was utilized.<sup>5</sup> The mass spectrometry ion source used was an electron bombardment source (EI), operating at 230 °C, while the quadrupole temperature was maintained at 150°C. For injection, the temperature of the injection port was set at 270°C, and high-purity helium gas was used as the carrier gas for chromatographic separation. The injection was performed in a splitless mode with 1 µL inject volume. The detection was conducted in both full scan mode (100-600 m/z) and selected ion mode.

### **Text S4. EPS desorption of BCCs-adsorbed PCB28**

After the adsorption equilibrium and centrifugation, 2 mL of supernatant were quickly replaced by the same volume of EPS solution. The sample vials were sealed and shaken (150 rpm, 30°C) for another 24 h to reach desorption equilibrium. Then, the PCB28 in the supernatant of the desorption solution was extracted and measured.

### **Text S5. Analysis of the interaction between TG9 and BCCs**

**Sample preparation for TEM observation.** After hydrophilic treatment of the copper mesh for 2 min, 20 µL of the co-culture solution was suspended on the copper mesh, and the excess liquid was sucked off from the edge of the mesh with the burr of the filter paper and waited for 10 s; 10 µL of phosphotungstic acid was dripped in, and the excess liquid was also sucked off with the same filter paper, and the sampling process was completed and ready for microscopic observation after waiting for 15 min.<sup>6</sup>

**Chemotactic experiment.** After cultivating TG9 in LB medium until the logarithmic phase, the

biomass was collected and washed twice with phosphate-buffered saline. The cells were then resuspended in M9 medium to achieve a final concentration of  $10^7$  cells/L, forming a cell suspension. M9 media containing 5 g/L BCCs were prepared as chemotaxis test solutions, with 3 mg/L chloramphenicol added to inhibit natural cell growth. Using a 1 mL syringe, 0.2 mL of the test solution was aspirated, and the syringe needle was wiped with sterile paper. The syringe was then inserted into the cell suspension (0.2 mL). After incubating at  $30^\circ\text{C}$  for 8 h, the liquid from the syringe was transferred to a centrifuge tube, and the cell concentration was diluted to  $10^4\sim 10^5$  cells/L using M9 medium. The number of cells that migrated into the test solution was determined using the plate count method, allowing for the calculation of the microbial chemotactic index  $I$ , as described in following equation.

$$I = \frac{Cell_t}{Cell_0}$$

where  $Cell_t$  represents the cell concentration (CFU/mL) in the test solution after  $t$  hours of chemotaxis towards BCCs, while  $Cell_0$  denotes the cell concentration (CFU/mL) in the test solution without BCCs.

**Protein gel electrophoresis.** Firstly, in the SDS-PAGE gel premixing solution (5%), the corresponding amount of 10% gel polymerisation catalyst solution was added according to the ratio of 1%, and the corresponding amount of tetramethylethylenediamine (TEMED) was added according to the ratio of 0.1%. The mixed solution was poured into the gel-making against the wall, followed by the insertion of a comb, and the gel-making process was completed by gently pulling out the comb after the gel had solidified.<sup>7</sup> The bacteria-BCCs mixture was added to the spiking frame, and the SDS mixture was selected as the electrophoresis solution, which was electrophoresed at 120 V for 15 min.

#### **Text S6. Determination of electron transfer activity**

**C-V curve measurement.** Ag/AgCl electrode was used as the reference electrode, platinum wire electrode as the counter electrode, BCCs-modified glassy carbon electrode as the working electrode, and inorganic salt medium was used as the electrolyte for the test. The scanning range was  $-1\sim 1$  V, and the scanning rate was  $0.1\text{ m Vs}^{-1}$ . A total of three rounds of scanning were performed to

take the results of the second round to exclude the false results caused by the instability of the instrument. The working electrode was modified as follows<sup>8</sup>: 200  $\mu\text{L}$  of BCCs suspension (10 ppm) was mixed with 50  $\mu\text{L}$  of Nafion, and 5  $\mu\text{L}$  of the suspension was placed on a polished glassy carbon electrode and placed in a fume hood until the BCCs powder adhered to the electrode surface.

**Electron transfer system activity measurement.** About 150  $\mu\text{L}$  of 0.5 wt% INT storage solution was added to 200  $\mu\text{L}$  of mixed culture solution of TG9 and BCCs, which was placed in the dark place to avoid light for incubation (30°C, 30 min) and followed by adding 40  $\mu\text{L}$  of formaldehyde solution to terminate the reaction. After the cells were collected by centrifugation (8000 rpm, 10 min), 500  $\mu\text{L}$  of methanol was added to extract the INF, and the process of ultrasonic-vortex extraction was repeated three times. The supernatants were combined, and then the absorbance was measured by an enzyme marker at 490 nm using methanol as a blank control.<sup>9</sup> In this experiment, we established two groups: the bacterial/BCCs alone exposure groups and the combined exposure group. This setup allows us to evaluate the effect of BCCs on electron transfer in the respiratory chain of bacteria by comparing absorbance, while also determining the interference from BCCs' adsorption effect by examining absorbance changes in the BCCs alone exposure groups. The exposure times set for this experiment were 0, 1, 2, 4, 6, 8 and 12 d.

**Table S1. Composition of the MSM medium.**

<b>Medium</b>	<b>Reagent</b>	<b>Concentration (g/L)</b>
<b>MSM medium</b>	$\text{KH}_2\text{PO}_4$	1
	$\text{K}_2\text{HPO}_4 \cdot 3\text{H}_2\text{O}$	3
	$\text{MgSO}_4$	0.5
	$\text{FeSO}_4$	0.02
	$\text{CaCl}_2$	0.02
	$\text{NaCl}$	1
	$(\text{NH}_4)\text{SO}_4$	0.5
	Micronutrient solution	1 mL
<b>Micronutrient solution</b>	$\text{Na}_2\text{MO}_4 \cdot \text{H}_2\text{O}$	6.7
	$\text{ZnSO}_4 \cdot 5\text{H}_2\text{O}$	28
	$\text{CuSO}_4 \cdot 5\text{H}_2\text{O}$	2.0
	$\text{H}_3\text{BO}_4$	4.0
	$\text{MnSO}_4 \cdot 5\text{H}_2\text{O}$	4.0
	$\text{CoSO}_4 \cdot 7\text{H}_2\text{O}$	4.7

**Note: pH=7.3**

**Table S2. Retention time and electron impact mass spectral characteristics of metabolites.**

Times	Mass	M/z (Relative strength)	Structural formula	Substance
30.532	430	344(100.00), 73(62.89), 360(40.19), 45(20.77), 376(19.42), 93(13.32)		3Cl-HOPDA
35.151	465	285(100.00), 329(38.54), 355(26.92), 183(33.20), 255(23.92)		2Cl-HOPDA
25.556	256	75(21.38), 93(14.08), 150(20.32), 186(55.83), 258(100.00)		PCB28
24.475	440	267(9.76), 247(79.95), 224(8.18), 159(5.46), 73(100)		Dichloro- dihydroxybenzoic acid
23.348	322	267(1.26), 247(45.10), 162(3.24), 97(5.49), 73(100)		Dichloro- dihydroxyphenol
22.687	351	351(0.53), 321(5.20), 247(31.65), 212(1.64), 177(9.29), 147(29.96),		Dichloro-hydroxybenzoic acid
21.895	222	71(30.91), 85(24.04), 111(8.40), 153(62.00), 186(2.62), 222(100.00)		4,4'-Dichlorobiphenyl
24.239	222	71(24.38), 85(26.11), 57(26.11), 153(94.56), 222(100.00)		2,4-Dichlorobiphenyl
19.346	262	109(19.86), 145(25.77), 173(40.05), 203(19.31), 247(100.00), 262(5.93)		Dichlorobenzoic acid
16.415	262	75(100), 247(37.44), 57(21.91), 85(9.90), 102(8.75)		2, 4-dichloro-alpha- methylbenzyl alcohol
16.230	228	75(27.72), 111(47.85), 139(59.94), 169(57.93), 213(100.00), 228(5.62)		Monochlorobenzoic acid

**Note: The mass numbers and fragment ions are the data corresponding to the TMS derivatives of the degradation products.**

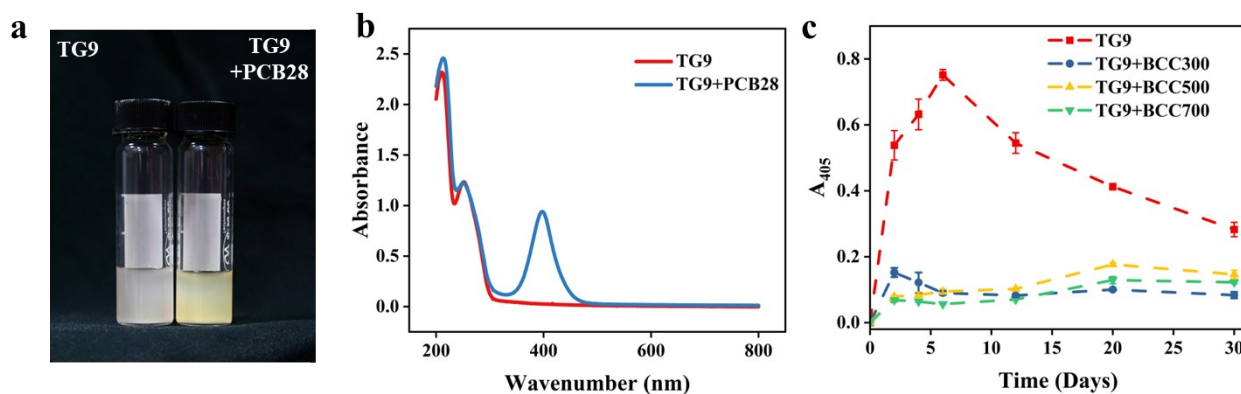


Figure S1. (a) Observation of solution color change after degradation of PCB28 by TG9; (b) UV spectra of yellow supernatants at 200-800 nm; (c) absorbance (at 405 nm) changes of water-soluble degradation products (nCl-HOPDA) in the different degradation systems.

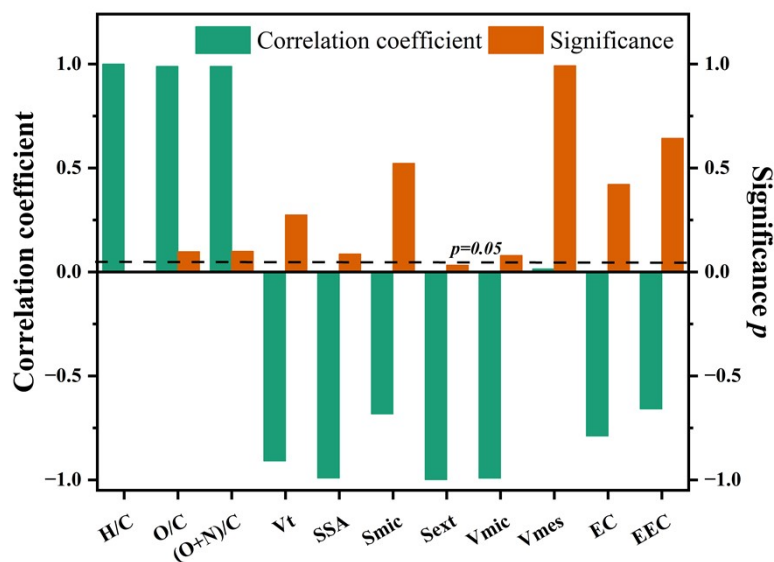
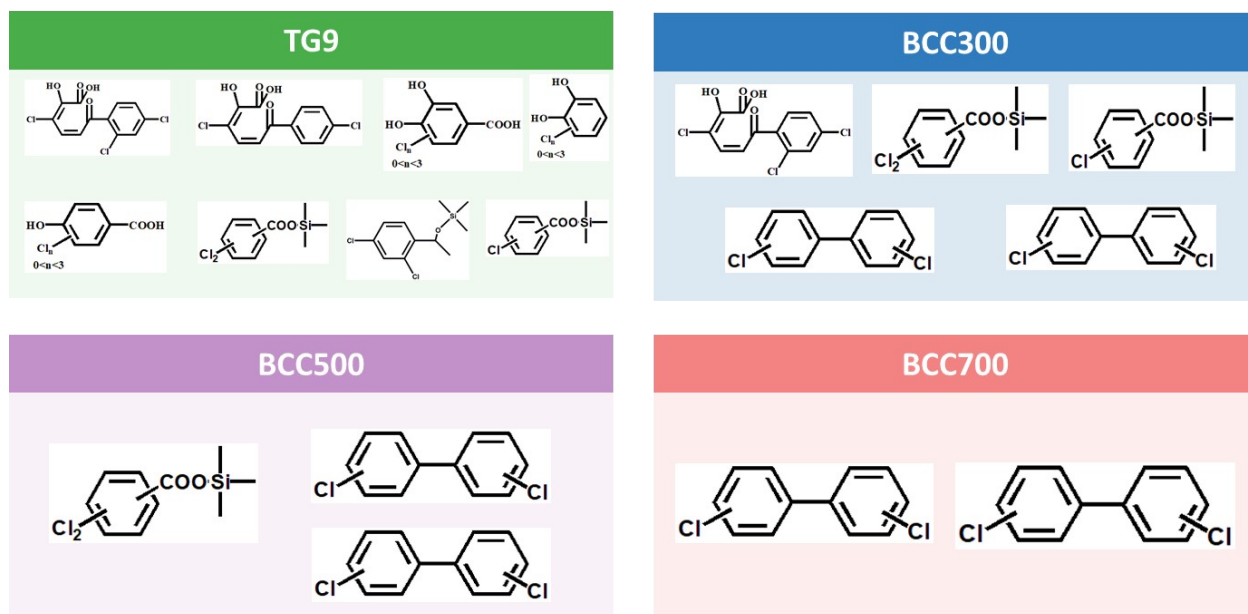
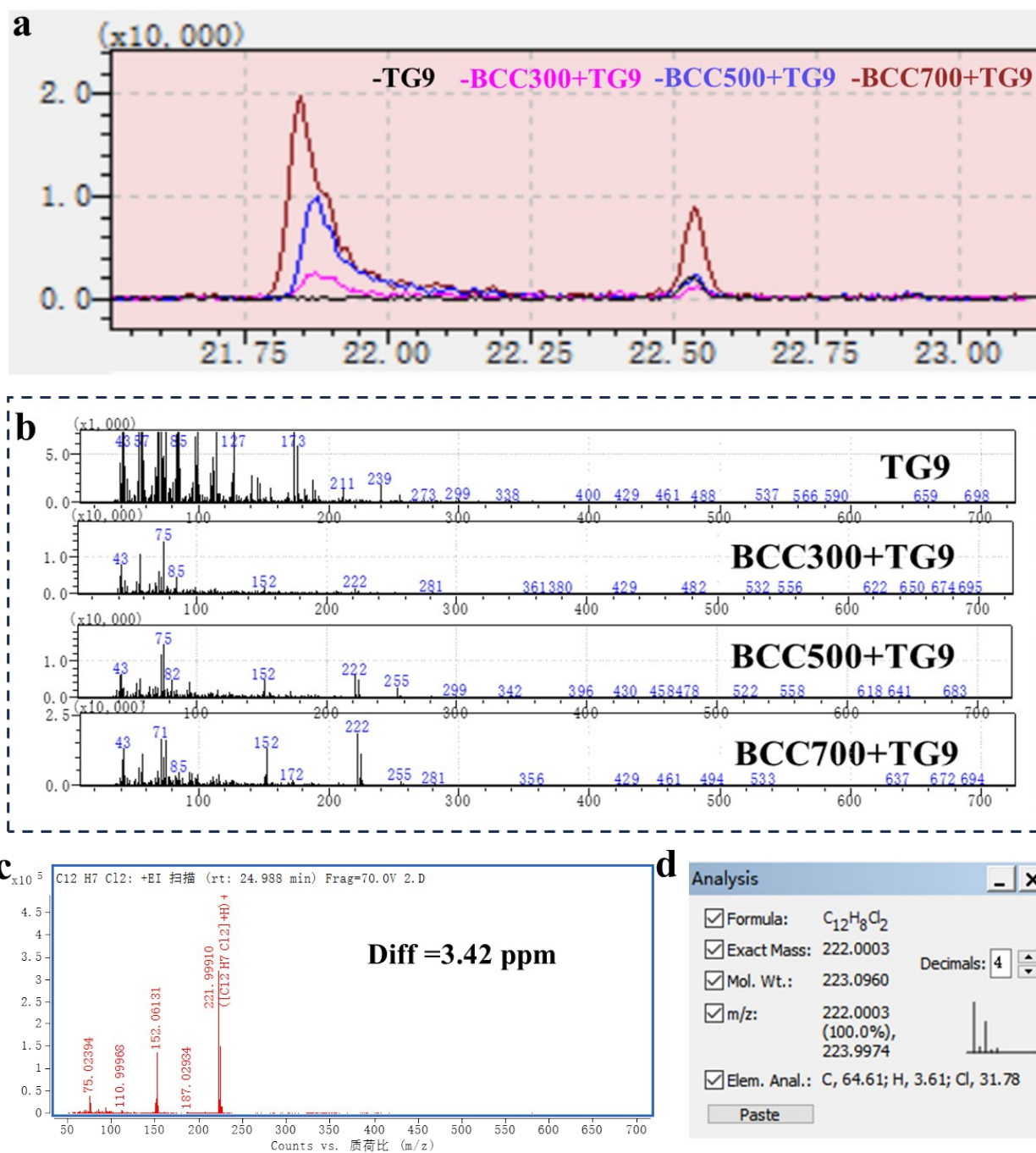


Figure S2 The relationships between the biodegradation rates ( $K_{obs}$ ) and physicochemical properties of BCCs. SSA: specific surface area;  $S_{ext}$ : external surface area;  $V_t$ : total pore volume;  $V_{mic}$ : micropore volume;  $V_{mes}$ : mesopore volume; EC: electric conductivity; EEC: electron exchange capacity.





**Figure S3.** The detected degradation products of PCB28 by TG9 alone and together with BCC300, BCC500 or BCC700.



**Figure S4.** Mass spectrometry analysis of the degradation product dichlorobiphenyl in the BCCs-PCB28 microbial degradation systems: (a) chromatogram, (b) mass spectrometry at 21.845 min, (c) high-resolution mass spectrometry of dichlorobiphenyl, and (d) theoretical molecular weights of dichlorobiphenyls.

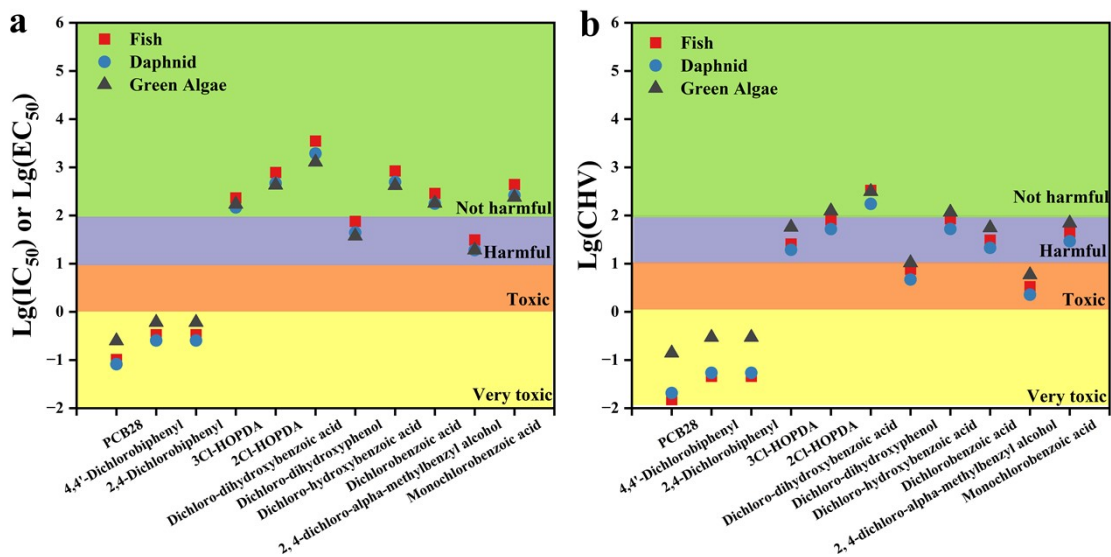


Figure S5. Acute (a) and chronic (b) aquatic toxicities of PCB28 and its degradation products to selected model aquatic organisms. IC<sub>50</sub> and EC<sub>50</sub> stand for the 50% inhibitory concentration and 50% effective concentration, respectively. CHV means chronic toxicity

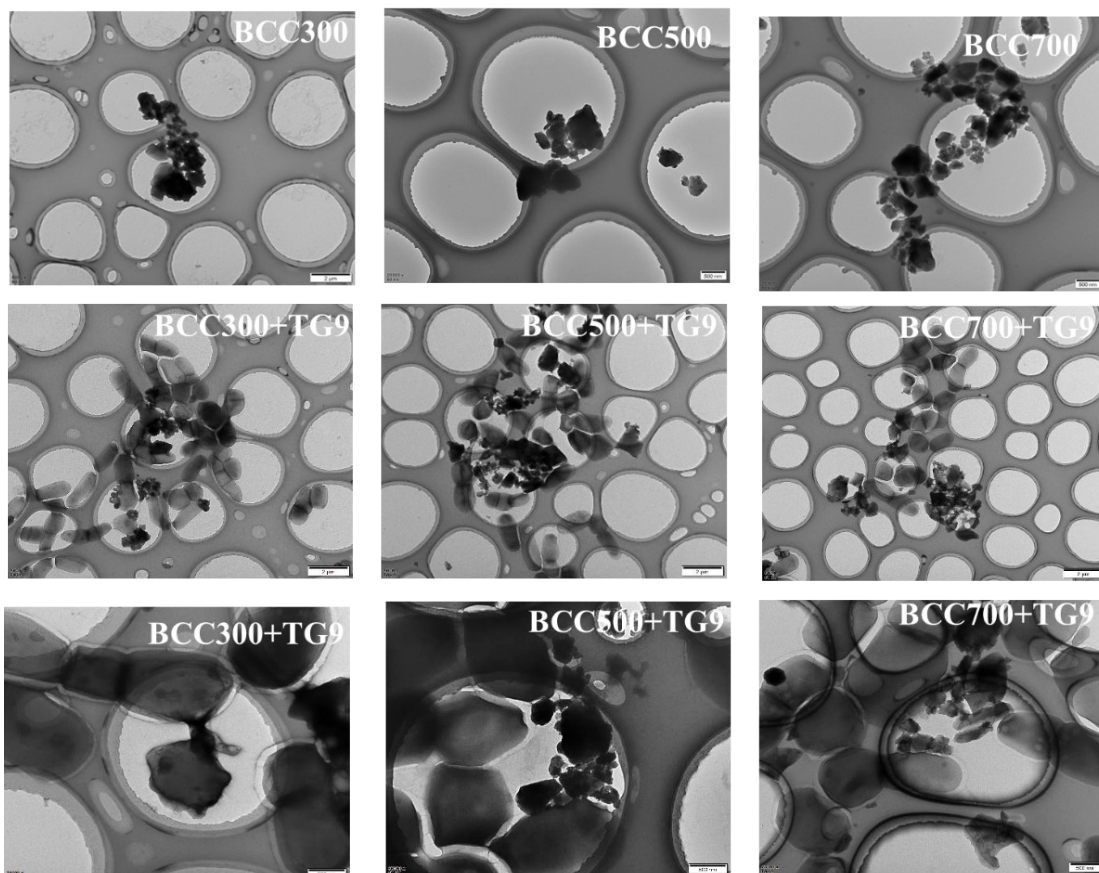


Figure S6. TEM images of BCCs along or together with TG9 after 10 days of co-culture. First row: pure BCCs, second row: BCCs and TG9, and third row: BCCs and TG9 (enlargement).

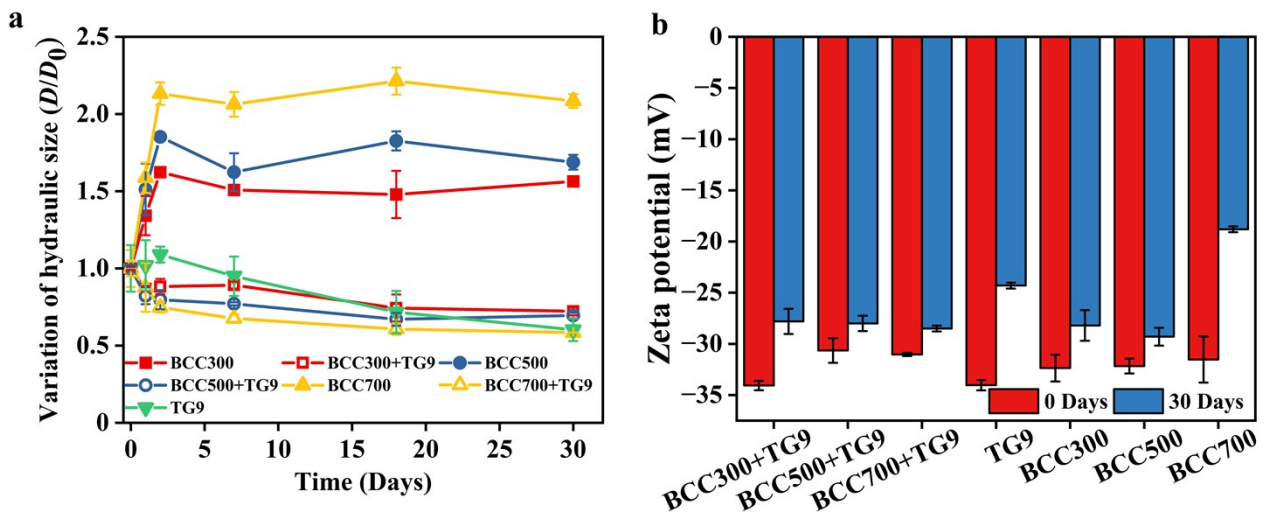


Figure S7. (a) Variations of the hydrodynamic size of BCCs with or without the TG9 treatment for different time; (b) the zeta potential of each treatment system after 30 days.

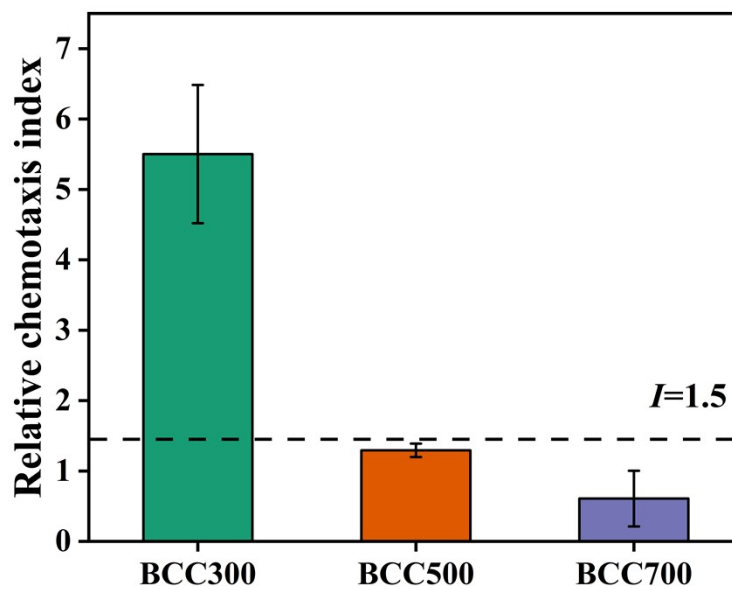


Figure S8. Capillary assays showing chemotaxis of TG9 towards BCCs.

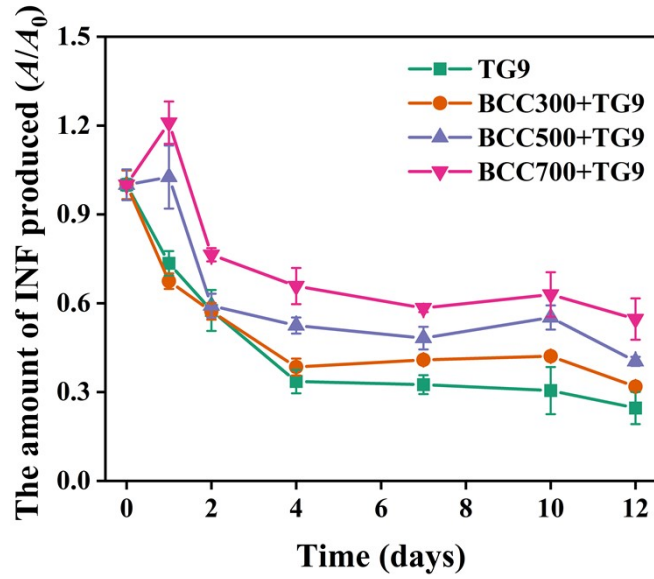


Figure S9. The kinetic curves of INF production by TG9 under co-culture conditions with and without BCCs.

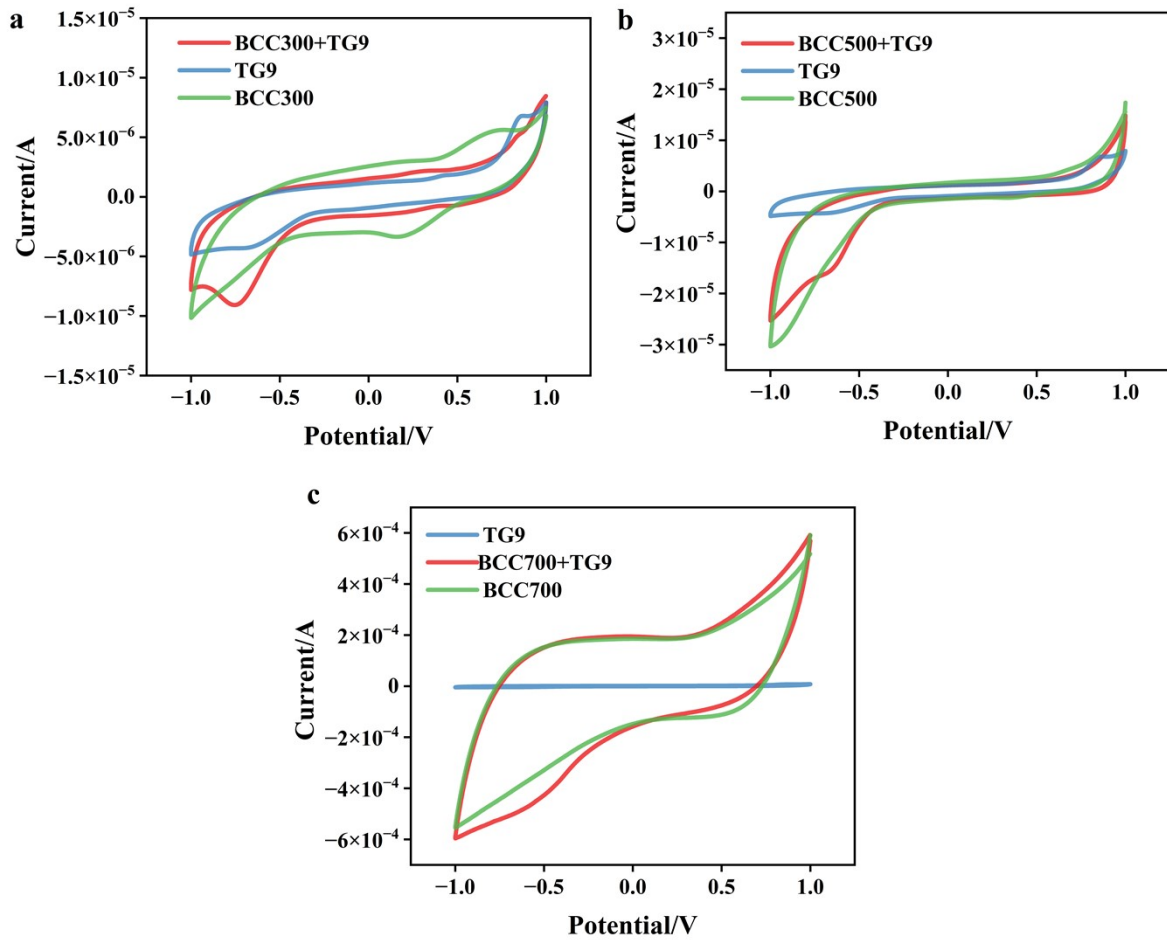


Figure S10. C-V curves of TG9 with (a) BCC300, (b) BCC500, and (c) BCC700.

## References

1. X. M. Su, Y. D. Liu, M. Z. Hashmi, J. X. Hu, L. X. Ding, M. Wu and C. F. Shen, *Rhodococcus biphenylivorans* sp nov. a polychlorinated biphenyl-degrading bacterium, *Anton Leeuw Int J G*, 2015, **107**, 55-63.
2. X. M. Su, L. Guo, L. X. Ding, K. Qu and C. F. Shen, Induction of viable but nonculturable state in *Rhodococcus* and transcriptome analysis using RNA-seq, *Plos One*, 2016, **11**, e0147593.
3. Z. M. Wang, K. Yang and D. H. Lin, Adsorption and desorption of polychlorinated biphenyls on biochar colloids with different pyrolysis temperatures: the effect of solution chemistry, *Environ Sci Pollut R*, 2023, **30**, 72966-72977.
4. T. Wu, Y. Z. Liu, T. Y. Zheng, Y. B. Dai, Z. Y. Li and D. H. Lin, Fe-based nanomaterials and plant growth promoting rhizobacteria synergistically degrade polychlorinated biphenyls by producing extracellular reactive oxygen species, *Environ Sci Technol*, 2023, **57**, (34), 12771–12781.
5. Z. M. Wang, X. T. Lin, K. Yang and D. H. Lin, Differential photodegradation processes of adsorbed polychlorinated biphenyls on biochar colloids with various pyrolysis temperatures, *Water Res*, 2024, **251**, 121174.
6. M. Kim, K. E. Lee, I. T. Cha and S. J. Park, *Draconibacterium halophilum* sp. nov. sp. nov., A halophilic bacterium isolated from marine sediment, *Curr Microbiol*, 2021, **78**, 2440-2446.
7. X. J. Cui, X. Y. Wang, X. L. Chang, L. Bao, J. G. Wu, Z. Q. Tan, J. M. Chen, J. Y. Li, X. F. Gao, P. C. Ke, C. Y. Chen and C. Murphy, A new capacity of gut microbiota: Fermentation of engineered inorganic carbon nanomaterials into endogenous organic metabolites, *P Natl Acad Sci USA*, 2023, **120**, e2218739120.
8. H. F. Wang, H. P. Zhao and L. Z. Zhu, Role of pyrogenic carbon in parallel microbial reduction of nitrobenzene in the liquid and sorbed phases, *Environ Sci Technol*, 2020, **54**, 8760-8769.
9. S. Y. Shen, W. N. Sun, K. Yang, H. C. Gao and D. H. Lin, Biotransformation of 2D nanomaterials through stimulated bacterial respiration-produced extracellular reactive oxygen species: A common but overlooked process., *Environ Sci Technol*, 2022, **56**, 5508-5519.